

AUS Repository

Modeling the Effects of Chemotherapy and Immunotherapy on Tumor Growth

Item Type	Article;Peer-Reviewed;Published version
Authors	El Haout, Sara;Fatani, Maymunah;Abu Farha, Nadia Khalil Mohammad;ALSawaftah, Nour Majdi;Mortula, Maruf;Husseini, Ghaleb
Citation	El Haout, S., Fatani, M., Abu Farha, N., ALSawaftah, N., Mortula, M., and Husseini, G. (2021). Modeling the Effects of Chemotherapy and Immunotherapy on Tumor Growth. Journal of Biomedical Nanotechnology,17(xx). doi:10.1166/jbn.2021.3214
DOI	10.1166/jbn.2021.3214
Publisher	American Scientific Publishers
Download date	2026-04-22 21:13:12
Link to Item	http://hdl.handle.net/11073/21581

Modeling the Effects of Chemotherapy and Immunotherapy on Tumor Growth

Sara El Haout¹, Maymunah Fatani¹, Nadia Abu Farha¹, Nour AlSawaftah²,
 Maruf Mortula³, and Ghaleb A. Hussein^{2, 4, *}

¹ Department of Electrical Engineering, American University of Sharjah, Sharjah, United Arab Emirates

² Material Science and Engineering Program, American University of Sharjah, Sharjah, United Arab Emirates

³ Department of Civil Engineering, American University of Sharjah, Sharjah, United Arab Emirates

⁴ Department of Chemical Engineering, American University of Sharjah, Sharjah, United Arab Emirates

Mathematical modeling has been used to simulate the interaction of chemotherapy and immunotherapy drugs intervention with the dynamics of tumor cells growth. This work studies the interaction of cells in the immune system, such as the natural killer, dendritic, and cytotoxic CD8+ T cells, with chemotherapy. Four different cases were considered in the simulation: no drug intervention, independent interventions (either chemotherapy or immunotherapy), and combined interventions of chemotherapy and immunotherapy. The system of ordinary differential equations was initially solved using the Runge-Kutta method and compared with two additional methods: the Explicit Euler and Heun's methods. Results showed that the combined intervention is more effective compared to the other cases. In addition, when compared with Runge-Kutta, the Heun's method presented a better accuracy than the Explicit Euler technique. The proposed mathematical model can be used as a tool to improve cancer treatments and targeted therapy.

KEYWORDS: Tumor Growth, Cancer, Chemotherapy, Immunotherapy, Ordinary Differential Equation.

INTRODUCTION

Cancer is the second most common cause of death in the United States, with approximately 1.9 million new cancer cases expected to be diagnosed (excluding basal cell and squamous cell skin cancers) and around 608,570 cancer-related deaths in 2021 [1]. Cancer is a complex metabolic disorder characterized by the uncontrolled growth and spread of abnormal cells. Although the causes of cancer are not completely understood, inherited genetic mutations and lifestyle factors (e.g., tobacco use, poor diet, and excess body weight) increase the risk of developing cancer. Currently, several methods can be used to treat cancer, including [2–6]:

- (1) Surgery works best for non-metastatic solid tumors. It can be used to remove the entire tumor, parts of the tumor, or ease cancer symptoms.
- (2) Chemotherapy uses drugs to stop or slow the growth of cancer cells. Although chemotherapy is a widespread

and effective way for cancer treatment, its main limitation is its non-specificity as chemotherapeutic agents attack both healthy and cancerous cells. Damage to healthy cells may cause side effects, such as mouth sores, nausea, and hair loss.

(3) Hormone therapy involves slowing or stopping the spread of cancers that use hormones to grow by blocking the body's ability to produce these particular hormones. This approach is prevalent for breast and prostate cancer.

(4) Immunotherapy works by boosting the patient's immune system. The immune system is a biological system that protects the organism against diseases and infections by identifying foreign matter such as tumor cells. Immunity can be innate or adaptive, with phagocytic cells such as lymphocytes, natural killer (NK) cells, dendritic cells (DCs), and cytokines all fall under the umbrella of innate immunity and are essential in tumor recognition. NK cells play a crucial role in destroying tumor cells before replication and growth, whereas DCs, also known as antigen-presenting cells (APC), help in activating the immune system by presenting antigens to CD8+ helper T cells that activate CD4+ helper T cells. Once activated,

* Author to whom correspondence should be addressed.

Email: ghusseini@aus.edu

Received: 25 September 2021

Accepted: 29 October 2021

CD4+ helper T cells secrete chemokines that enhance the immune response. Immunotherapy helps these elements of the immune system to better act against cancer.

(5) Radiation therapy uses high doses of radiation to kill cancerous cells and shrink tumors.

(6) Stem cell transplant can help cancer patients recover their ability to produce stem cells after treatment with very high doses of radiation therapy, chemotherapy, or both. It is also a recommended approach when dealing with blood-related cancers, such as leukemia, due to the graft-versus-tumor effect that can occur after allogeneic transplants. Graft-versus-tumor occurs when white blood cells (WBCs) from the donor (the graft) attack any cancer cells that remain in the graft-recipient's body after high-dose treatments.

(7) Targeted therapy is a type of cancer treatment that targets proteins that control how cancer cells grow, divide, and spread. Most targeted therapies involve either small-molecule drugs or monoclonal antibodies (mAbs).

Modeling of Tumor Growth

Several tumor-growth models have been developed to better understand the dynamics and evolution of tumors. Many studies applied ordinary differential equations (ODEs) to describe changes in the tumor burden (e.g., tumor volume, tumor size) and drug effect, allowing the rationalization of personalized treatments for cancer patients and overcoming cancer drug resistance. Basic mathematical functions such as linear, exponential, logistic, Gompertz, or a combination of exponential and linear models are commonly used to characterize natural tumor growth. The growth rate is assumed to be constant in linear models but proportional to tumor burden in exponential models. Real-life biological changes in the tumor growth rate can be represented with logistic and Gompertz models, where the Gompertz model considers the reduction of growth rate with time. In contrast, the logistic model considers the environment's carrying capacity, which limits the growth. Basic functions from previous work describing natural tumor growth are presented below, where k_g and d represent the growth rate and death rate constants, respectively; T represents tumor burden, and T_{\max} is the carrying capacity.

Linear growth

$$\begin{aligned} \frac{dT}{dt} &= k_g \\ \frac{dT}{dt} &= k_g - d \cdot T \end{aligned} \quad (1)$$

Exponential growth

$$\begin{aligned} \frac{dT}{dt} &= k_g \cdot T \\ \frac{dT}{dt} &= k_g \cdot T - d \cdot T \end{aligned} \quad (2)$$

Logistic growth

$$\frac{dT}{dt} = k_g \cdot T \cdot \left(1 - \frac{T}{T_{\max}}\right) \quad (3)$$

Gompertz growth

$$\frac{dT}{dt} = k_g \cdot T \cdot \ln\left(\frac{T_{\max}}{T}\right) \quad (4)$$

More advanced models incorporate additional parameters such as drug concentration, tumor shrinkage rate constant, time, location, etc. Some ODE models incorporate biological factors and processes, including the relationship between the immune system (e.g., cytotoxic T lymphocytes) and the cancer growth rate of patients undergoing immunotherapy. Such model-based approaches provide an opportunity to better understand cancer evolution, investigate treatment optimization, overcome cancer drug resistance, and even predict tumor dynamics [7]. Currently, there is a growing trend towards the use of fractional calculus to model tumor behavior [8–10]. Fractional models are characterized by an arbitrary order of differentiation or integration, and have inherent attributes that may improve ODE-based tumor models.

Tumor Growth Modelling for Chemotherapy

Chemotherapy is defined as the use of drugs to kill cancer cells. Many studies have investigated the response of different cancer types to various chemotherapeutic agents. Peng et al. [11] conducted a study focused on evaluating the performance of quantitative contrast-enhanced ultrasonography (CEUS) to assess the response of a cervical tumor to neoadjuvant chemotherapy (NACT). The CEUS model compared different parameters related to tumor response, such as maximum intensity (IMAX), rise time (RT), time-to-peak (TTP), and mean transit time (MTT). These parameters were compared between the cervical tumor and myometrium (reference zone) using a software called Sonolive. The study reported that the quantitative CEUS showed significant changes in cervical tumor perfusion after one cycle of NACT; for example, a considerable decrement was observed for the IMAX correlated with better tumor perfusion response. In another study, Patwardhan et al. [12] discussed multidrug resistance (MDR) as one of the major obstacles that limit the success of cancer chemotherapy. The study adopted a Flutax-2 and spectrometry model to directly measure the cellular efflux of tumors *in vivo*. It was thought that this approach would provide a better estimation of the cellular flux than the estimation of MDR1 mRNA and P-glycoprotein levels in samples stored or embedded. The study characterized drug resistance to decide on the best drug for cancer patients. Results showed that the study successfully measured cellular transportability, including efflux and accumulation for various cancer types; for example, the analysis successfully detected an increment in the accumulation and

a decrement in the efflux of NCI/ADR-RES cells treated with verapamil.

Zhao et al. [13] evaluated the predictive value of immunohistochemical or fluorescence *in situ* hybridization (HER IHC or FISH) positivity in tumor response to HER2 targeted therapy. The experiment was performed by taking biopsies of 76 HER2+ breast cancer patients who had received chemotherapy and neoadjuvant HER2 targeted therapy. The results of the univariate analysis showed that some characteristics of the tumor (small size, low nuclear grade, high Ki67, HER2 IHC 3+, homogenous strong HER2 IHC staining, high HER2/CEP17 ratio, and high HER2 copy number) are highly associated with pCR/RCB-I which led them to the conclusion that the HER2 IHC pattern is highly associated with tumor response to neoadjuvant chemotherapy. Anaya et al. [14] evaluated chemotherapy concentration at the tumor site and the associated treatment response for patients with colorectal cancer liver metastases, using a mathematical model. Results showed that the estimated tumor-site chemotherapeutic concentration (eTSCC) decreased with a quadratic decrement from TRG = 1 to TRG = 5 ($p < 0.001$). In addition, Koziol et al. [15] used a dynamic model of cancer growth using three types of interacting cell populations: tumor cells, healthy host cells, and immune effector cells. The model of tumor growth took into consideration the heterogeneity of the tissue based on the interaction between various cell types. The results showed that there is a correlation between theoretical and empirical knowledge of tumor growth. The study used an explicit delay differential equation model to show the major features of the Simeoni ODE model by evaluating mammary tumor growth in mice. The study reported that the Simeoni tumor growth function alters between exponential and linear growth where the alteration did not pass any plateau phase. Aghaei et al. [16] employed a dataset for breast MR images of 151 cancer patients before neoadjuvant chemotherapy was used. Patients had received either a complete response (CR) or a partial response (PR) to chemotherapy based on the RECIST criterion. A computer-aided detection (CAD) scheme and an artificial neural network (ANN) were used to differentiate between the CR and PR cases. The results showed that high accuracy was obtained using ten different features for the classification between CR and PR. Finally, Ledzewicz et al. [17] employed a Gompertz growth model for cancer cells and calculated the optimal control and corresponding responses. The study targeted reducing the tumor volume by giving small dosages. Results showed that the PR provided better responses as it led to tumor volume shrinkage.

Tumor Growth Modelling for Chemotherapy and Immunotherapy

Immunotherapy treatment relies on enhancing the immune system in such a way that it is capable of identifying and

killing tumor cells. Some research studies have combined both chemotherapy and immune therapy to enhance the tumor response to treatment. Alvarez et al. [18] proposed a nonlinear mathematical model to simulate the response of cancer to immunotherapy based on the phenotypic heterogeneity of tumor cells and the differences in immunogenicities. The study examined the effect of immunotherapy on the expression of cell surface receptors, growth, angiogenic, proliferative, and immunogenic factors. The model adopted by this study revealed a phenomenon related to tumor dormancy, robustness, immunoselection over tumor heterogeneity, referred to as “cancer immunoediting.” The adopted model also helped quantitatively describe cancer immunoediting within the context of sensitivity to the initial conditions, which helped quantify some of the mechanisms underlying tumor dynamics. Admon et al. [19] developed a mathematical model to study, predict, and control tumor growth. The ODEs used in this study modeled the effect of combining immunotherapy and certain anticancer drugs on tumor cells, with a special focus on the stability analysis at the tumor site. Specific parameters that reflect the stability of the tumor after treatment were measured, and the results showed that when the combinational treatment was administered, the tumor growth region decreased, and tumor cells in the interphase and metaphase stages of the cell cycle decreased by 1.27% and 1.53%, respectively. Moreover, Pinho et al. [20] utilized a model based on five ODEs to study the interactions between normal cells, cancer cells, endothelial cells, chemotherapeutic agents, and anti-angiogenic agents in tumor growth. The study reported that combining anti-angiogenic and chemotherapeutic agents helped slow down cancer growth and led to a larger reduction in tumor size than with chemotherapy alone.

Unni and Seshaiyer [21] developed a mathematical model to study the interactions between tumor and immune cells (NK cells, DCs, and cytotoxic CD8+ T cells). The analysis focused on the effect of immunotherapy and chemotherapy on tumor growth. Stability analysis results conducted on this model provided insight into the interactions between tumor cells, the immune system, and drug response systems. The study also reported that the joint use of tumor-infiltrating lymphocytes (TIL) therapy and chemotherapy played an essential role in controlling tumor growth. Robertson-Tessi et al. [22], developed a model to quantitatively assess the effect of the adaptive immune system on anti-tumor chemotherapy or chemioimmunotherapy. The adopted model examined the interaction between tumors and the adaptive immune system, in addition to the controllability of tumors through the interplay of cytotoxic, cytostatic, and immunogenic effects of chemotherapy. The changes in the growth rate and antigenicity were studied by examining cytotoxic and helper T cells, T regulatory cells (T_{regs}), DCs, memory cells, and several key cytokines. The study reported that the

tumor response to treatment depends entirely on the balance between immunosuppressive and immunostimulatory effects. The response can alter based on innate tumor characteristics such as growth rate and antigenicity. Curtis and Frieboes [23] developed a model to evaluate the response of tumors to the combination of chemotherapy and immunotherapy, focusing on non-small cell lung cancer (NSCLC). The parameters were set to simulate a NSCLC nodule being treated with paclitaxel (PTX). Their findings showed that the system was capable of exploring variations in therapy parameters, including dosing, drug strength, and effect, and their combination across various immuno- and chemotherapeutics.

The purpose of this study is to simulate four cases of tumor growth: with chemotherapy, with immunotherapy, with both chemotherapy and immunotherapy, and without any drug intervention. Three different approaches were used to solve the ODEs. The original approach obtained from literature is assumed to be the optimal approach, while the two other methodologies will be compared with the actual outcome.

METHODOLOGY

In this study, we mathematically modeled the interaction between growing tumor cells and the immune system. Our models considered four cell populations: tumor cells $T(t)$, natural killer cells $N(t)$, dendritic cells $D(t)$, and cytotoxic CD8+ T cells $L(t)$. We selected these immune cells because they are the most relevant in cancer immunotherapy; NK cells and CD8+ T-cells are known to kill tumor cells, while dendritic cells are antigen-presenting cells that help stimulate and activate the immune system [21, 24]. Incorporating each cell type involved in fighting cancer would be ideal; however, this would lead to extremely complex models that would be computationally costly [25]. The ODEs used to express the dynamic changes of those parameters over time were obtained from literature as follows:

$$\frac{dT}{dt} = aT(1 - bT) - (c_1N - jD + kL)T - K_T z(M)T \quad (5)$$

$$\frac{dN}{dt} = s_1 + \frac{g_1NT^2}{h_1 + T^2} - (c_2T - d_1D)N - K_N z(M)N - eN \quad (6)$$

$$\frac{dD}{dt} = s_2 - (f_1L + d_2N - d_3T)D - K_D z(M)D - gD \quad (7)$$

$$\frac{dL}{dt} = f_2DT - hLT - uNL^2 + r_1NT + \frac{p_1LI}{g_1 + I} - K_L z(M)L - iL + v_L \quad (8)$$

$$\begin{aligned} \frac{dM}{dt} &= v_M(t) - d_4M \\ \frac{dI}{dt} &= v_I(t) - d_5I \end{aligned} \quad (9)$$

The five ODEs presented above have been used in modeling tumor growth. The following sections will explain the components of each equation. The ODEs presented above could be related in real life; however, for the sake of simplifying the model, the interactions between these cell populations are out of the scope of this analysis.

Modeling Tumor Cells

As mentioned earlier, biological models can be best represented by a logistic growth model $aT(1 - bT)$, where a and b denote the growth of tumor cells impacted by the interactions of N , D , and L with tumor cells, separately. Equation (5) includes the competition term $-(c_1N + jD + kL)T$, where j is the interaction between T and D cells, c_1 is the interaction between T and N , while k is the interaction between T and L , the estimated values of which are presented in Table I. In general, the effect of a chemotherapeutic drug is found by multiplying the value of the kill parameter $K_{[]}$ by $z(M)$, which represents the effectiveness of the drug during certain cell cycle phases.

Table I. Description and value of parameters.

Parameter (unit)	Description	Estimated value
a (day ⁻¹)	Tumor growth rate	4.31×10^{-1}
b (cells ⁻¹)	Tumor-carrying capacity estimated	2.17×10^{-8}
c_1 (cells ⁻¹)	NK cell tumor cell kill rate estimated	3.5×10^{-6}
c_2 (cells ⁻¹ day ⁻¹)	NK cell inactivation rate by tumor cells	1.0×10^{-7}
d_1 (cells ⁻¹)	Rate of dendritic cell priming NK cells	1.0×10^{-6}
d_2 (cells ⁻¹)	NK cell dendritic cell kill rate	4.0×10^{-6}
d_3 (cells ⁻¹)	Rate of tumor cells priming dendritic cells	1.0×10^{-4}
e (day ⁻¹)	Death rate of NK cell	4.12×10^{-2}
f_1 (cells ⁻¹)	CD8+ T cell dendritic cells kill rate	1.0×10^{-8}
f_2 (cells ⁻¹)	Rate of dendritic cells priming CD8+ T cell	0.01
g (cells ⁻¹)	Death rate of dendritic cells	2.4×10^{-2}
h (cells ⁻¹ day ⁻¹)	CD8+ T inactivation rate by tumor cells	3.42×10^{-10}
i (day ⁻¹)	Death rate of CD8+ T cells estimated	2.0×10^{-2}
j (cells ⁻¹)	Dendritic cell tumor kill rate	1.0×10^{-7}
k (cells ⁻¹)	NK cell tumor cell kill rate	1.0×10^{-7}
s_1 (cells ⁻¹)	Source of NK cells	1.3×10^4
s_2 (cells ⁻¹)	Source of dendritic cell	4.8×10^2

By default, when there is no drug administered or no tumor present, $(dT/dt) = 0$.

Modeling Natural Killer Cells

NK cells are assumed to have a constant source (s_1). To model these cells (as seen in Eq. (6)), the parameters g_1 and h_1 expressing the recruitment of N by T cells are considered. In addition, the growth of N cells while being impacted by T cells with a kill rate (c_2), and by D cells with a kill rate (d_1) are also considered; along with the natural death of N ($-eN$).

Modeling Dendritic Cells

Dendritic cells with a constant source of D cells (s_2) also interact with L cells (f_1), and proliferate with the tumor (d_3). The death of these cells by N cells is denoted by d_2 and g , respectively. All of these parameters are expressed in Eq. (7) to model D cells.

Modeling Cytotoxic CD8+ T Cells

Cytotoxic CD8+ T cells are tumor-specific cells that play a major role in the immune system in the presence of tumors. These cells are activated via an interaction rate of D and T (f_2), and naturally die at a rate of ($-iL$). The concentration of immunotherapy drug in the bloodstream is denoted by (I), in which the activation of L cells by IL-2 immunotherapy is described as: $(p_1LI)/(g_1 + I)$. Equation (8) models the L cells, where the second term ($-hLT$) represents the competitive interaction between L and T cells, the third term (uNL^2) describes changes in D cell activity and levels, while the (r_1NT) term describes D cells recruitment.

Modeling Drugs and Vaccine Intervention

The administration of immunotherapy through TIL drugs is denoted by v_L , which is included in Eq. (8), while chemotherapy drug intervention is denoted by v_M . The elimination of immunotherapy and chemotherapy drugs from the body over time is expressed in Eq. (9) as d_5I and d_4M , respectively. The dynamics of the concentration of drugs in the bloodstream are given by $dM/dt = v_M(t) - d_4M$, for chemotherapy, and $dI/dt = v_I(t) - d_5I$ for immunotherapy.

Stability Analysis

When there is no drug intervention, Eqs. (5)–(8) will be equal to zero at the equilibrium point. At tumor-free conditions ($T = 0$), Eq. (6) becomes:

$$N^* = \frac{s_1}{e - d_1D^*} \quad (10)$$

where $e - d_1D^* > 0$

Since CD8+ T cells are only activated where there is a tumor; therefore, Eq. (6) becomes:

$$N = \frac{gD^* - s_2}{d_2D^*} \quad (11)$$

By substituting (10) and (11), the resulting equation is:

$$\frac{s_1}{e - d_1D^*} = \frac{gD^* - s_2}{d_2D^*}$$

$$gd_1D^{*2} - (s_2d_1 + d_2s_1 + eg)D^* + es_2 = 0$$

To solve for D , use the quadratic formula where $a = gd_1$, $b = d_1s_2 + d_2s_1 + eg$, and $c = es_2$

$$D_{1,2}^* = \frac{(d_1s_2 + d_2s_1 + eg) \pm \sqrt{(d_1s_2 + d_2s_1 + eg)^2 - 4ges_2}}{2gd_1} \quad (12)$$

where $d_1s_2 + d_2s_1 + eg \geq \sqrt{4ges_2}$

To match real-life conditions, $e - d_1D^* > 0$ and $d_1s_2 + d_2s_1 + eg \geq \sqrt{4ges_2}$. This condition satisfies Eqs. (11) and (12). In other words, under tumor-free equilibrium conditions, the critical points for NK cells' death rate, e , and the source term are:

$$e = d_1D^*$$

$$s_1 = \frac{\sqrt{4ges_2} - (d_1s_2 + eg)}{d_2} = \frac{2\sqrt{ges_2} - (d_1s_2 + eg)}{d_2}$$

Linearization of the ODE System

To linearize the system of ODEs presented above without drug intervention, a Jacobian matrix was used.

$$\begin{bmatrix} a_{11} & a_{12} & a_{13} & a_{14} \\ a_{21} & a_{22} & a_{23} & a_{24} \\ a_{31} & a_{32} & a_{33} & a_{34} \\ a_{41} & a_{42} & a_{43} & a_{44} \end{bmatrix}$$

From Eq. (5):

$$a_{11} = a - 2abT^* - c_1N^* - jD^* - kL^*$$

$$a_{12} = -c_1T^*$$

$$a_{13} = jT^*$$

$$a_{14} = -kT^*$$

From Eq. (6):

$$a_{21} = \frac{2g_1N^*h_1T^*}{(h_1 + T)^2} - c_2N^*$$

$$a_{22} = -c_2T^* + d_1D^* - e$$

$$a_{23} = d_1N^*$$

$$a_{24} = 0$$

From Eq. (7):

$$\begin{aligned} a_{31} &= d_3 D^* \\ a_{32} &= -d_2 D^* \\ a_{33} &= -(f_1 L^* + d_2 N^* - d_3 T^* + g) \\ a_{34} &= -f_1 D^* \end{aligned}$$

From Eq. (8):

$$\begin{aligned} a_{41} &= f_2 D^* - h L^* + r_1 N^* \\ a_{42} &= u D^{*2} + r_1 T^* \\ a_{43} &= f_2 T^* \\ a_{44} &= -(h T^* + 2u N^* L^* + i) \end{aligned}$$

Considering the equilibrium tumor-free critical points, the matrix elements that will equal zero are: a_{12} , a_{13} , a_{14} , a_{24} , a_{42} , and a_{43} . The remaining elements are calculated and arranged in matrix A .

$$A = \begin{bmatrix} a - c_1 N^* - j D^* & 0 & 0 & 0 \\ \frac{2g_1 N^* h_1 T^*}{(h_1 + T)^2} - c_2 N^* & d_1 D^* - e & d_1 N^* & 0 \\ d_3 D^* & -d_2 D^* & -(d_2 N^* + g) & -f_1 D^* \\ f_2 D^* + r_1 N^* & 0 & 0 & -i \end{bmatrix}$$

Where,

$$B = \begin{bmatrix} d_1 D^* - e & d_1 N^* \\ -d_2 D^* & -(d_2 N^* + g) \end{bmatrix}$$

The determinant must be calculated to find the eigenvalues λ , where $\det(A - \lambda I) = 0$

$$\det \begin{bmatrix} a - c_1 N^* - j D^* - \lambda & 0 & 0 & 0 \\ \frac{2g_1 N^* h_1 T^*}{(h_1 + T)^2} - c_2 N^* & d_1 D^* - e - \lambda & d_1 N^* & 0 \\ d_3 D^* & -d_2 D^* & -(d_2 N^* + g) - \lambda & -f_1 D^* \\ f_2 D^* + r_1 N^* & 0 & 0 & -i - \lambda \end{bmatrix}$$

Yielding:

$$(a - c_1 N^* - j D^* - \lambda)(-i - \lambda)\det(B - \lambda I) = 0$$

The trace and determinant for matrix B are:

$$\text{tr}(B) = (d_1 D^* - e) - (d_2 N^* + g)$$

$$\det(B) = d_1 d_2 N^* D^* - (d_1 D^* - e)(d_2 N^* + g)$$

The eigenvalues are: $\lambda_1 = a - c_1 N^* - j D^*$ and $\lambda_2 = -i$, where $\lambda_1 < 0$ to stabilize the tumor-free equilibrium, and λ_3 and λ_4 are the roots of the equation:

$$\begin{aligned} \lambda^2 - \lambda[(d_1 D^* - e) - (d_2 N^* + g)] + d_1 d_2 N^* D^* \\ - (d_1 D^* - e)(d_2 N^* + g) = 0 \end{aligned}$$

Or $\lambda^2 - \text{tr}(B)\lambda + \det(B) = 0$

Since $e - d_1 D^* > 0$, then the trace and determinant for matrix B should satisfy the conditions: $\text{tr}(B) < 0$ and $\det(B) > 0$.

ODE Methods Used

Runge-Kutta 4th Order Method

This numerical method consists of an *ODE* that defines the value of (dT/dt) with an initial value of $t(0) = t_0$. The goal is to find an unknown value function t at any given point T , where t represents time and T represents the number of tumor cells under different scenarios, such as no drug administered, immunotherapy alone, chemotherapy alone, and the combination of immunotherapy and chemotherapy. As seen below, formulas are used to compute the next value of T_{i+1} from the previous value T_i . The values of $= 0, 1, 2, 3 \dots (t - t_0)/\Delta t$, where Δt is a time step and $\Delta t = T_{i+1}/T_0$.

$$T_{i+1} = T_i + \frac{1}{6}(\Delta T_1 + 2\Delta T_2 + 2\Delta T_3 + \Delta T_4)$$

$$\Delta T_1 = \Delta t f(t_i, T_i)$$

$$\Delta T_2 = \Delta t f\left(t_i + \frac{\Delta t}{2}, T_i + \frac{\Delta T_1}{2}\right)$$

$$\Delta T_3 = \Delta t f\left(t_i + \frac{\Delta t}{2}, T_i + \frac{\Delta T_2}{2}\right)$$

$$\Delta T_4 = \Delta t f(t_i + \Delta t, T_i + \Delta T_3)$$

T_1 presents the slope at the beginning of the interval (Euler), T_2 presents the slope at the midpoint of the interval between t and T_1 , T_3 presents the slope at the midpoint of the interval between t and T_2 , while T_4 presents the slope at the end of the interval. In our analysis, we used the built-in MATLAB function ODE45, where the local error is on the order of $O(h^5)$ while the total error accumulates on the order of $O(h^4)$.

Explicit Euler Method

Using the forward finite difference $O(h)$, is the best way to present a time-independent variable, keeping in mind that the obtained solution will not give an exact result but will provide specific T values for all grid points Δt . As seen below, Eq. (13) was used to compute the solution using T_i where $T_i \equiv T(t = t_i)$. The step size Δt was assumed to be constant as a simplification and was then given by $\Delta t = t_i - t_{i-1}$.

$$\frac{T_{i+1} - T_i}{\Delta t} = f(T_i, t_i) \tag{13}$$

Although the Explicit Euler is the simplest method for solving 1st order differential equations, it is limited by being conditionally stable. To resolve this issue, setting $|G| \leq 1$ will render it stable. Using Eq. (14), we computed the condition for Explicit Euler to be stable by;

$$\frac{T_{i+1} - T_i}{\Delta t} = -\alpha T_i \tag{14}$$

$$T_{i+1} = -\alpha T_i \Delta t + T_i \text{ (common factor)}$$

$$T_{i+1} = (1 - \alpha \Delta t) T_i$$

G (amplification factor)

$$G \leq 1 \text{ or } \alpha \Delta t \leq 2$$

Heun's Method

Heun's method is based on Euler's method [26]; however, the latter provides a higher accuracy in comparison with the Euler explicit, which will be proven below in Figure 2.

Heun's method improves the slope estimation and involves the determination of two derivatives for the interval, one at each start point and endpoint. Then, the two derivatives are averaged to obtain an improved estimate of the slope.

```

clearvars
close all
clc
%% system parameters
a = 4.31e-1 % 1/day
b = 2.17e-8 % 1/cells
c1 = 3.5e-6 % 1/cells
c2 = 1e-7 % 1/cells/days
d1 = 1e-6 % 1/cells
d2 = 4e-6 % 1/cells
d3 = 1e-4 % estimate
e = 4.12e-2 % 1/day
f1 = 1e-8 % 1/cells
f2 = 1e-2 % 1/cells
g = 2.4e-2 % 1/cells
h = 3.42e-10 % 1/cells/days
i = 2e-2 % 1/day
j = 1e-7 % 1/cells
k = 1e-7 % 1/cells
s1 = 1.3e4 % 1/cells
s2 = 4.8e2 % 1/cells
z = @(M) 1-exp(-M) % chemotherapy effectiveness
vL_range = [0 1 0 1]*1e5; % TIL drug
vM_range = [0 1 1 1]; % chemotherapy drug
% influence of chemotherapy drug
KT_range = [0 0 1 1]*9e-2;
KN_range = [0 0 1 1]*6e-2;
KD_range = [0 0 1 1]*6e-2;
KL_range = [0 0 1 1]*6e-2;
%% input parameters
Tmax = 10 % maximum number of days
t = linspace(0,Tmax,20) % time discretization
y0 = [100;0;0;0;0] % initial data
%% case 2 model
% loop over d3 values
for id=1:length(vL_range)
    vL = vL_range(id) % variation of vL
    vM = vM_range(id) % variation of vM
    KT = KT_range(id) % variation of KT
    KN = KN_range(id) % variation of KN
    KD = KD_range(id) % variation of KD
    KL = KL_range(id) % variation of KL
    % model corresponding to d3
    dydt = @(t,y) [a*y(1).*(1-b*y(1))-(c1*y(2)+j*y(3)+k*y(4)).*y(1)-KT*z(y(5)).*y(1);
        s1-(c2*y(1)-d1*y(3)).*y(2)-KN*z(y(5)).*y(2)-e*y(2);
        s2-(f1*y(4)+d2*y(2)-d3*y(1)).*y(3)-KD*z(y(5)).*y(3)-g*y(3);
        f2*y(3).*y(1)-h*y(4).*y(1)-KL*z(y(5)).*y(4)-i*y(4)+vL;
        vM];
    %% ode solver
    [~,y1] = ode45(dydt,t,y0);
    y2 = expliciteuler(dydt,t,y0);
    y3 = heun(dydt,t,y0);
    %% extract results
    T1(:,id) = y1(:,1) % Tumor cells
    T2(:,id) = y2(:,1) % Tumor cells
    T3(:,id) = y3(:,1) % Tumor cells
end
% Error
Err1 = abs((T1 - T2)./T1)*100

```

Figure 1. MATLAB code used to conduct analysis.

It is a modified Euler with $T^{\text{predictor}}$ based on the explicit method and a $T^{\text{corrector}}$ that presents a generic equation:

$$T_{i+1}^c = T_i + \frac{\Delta t}{2}(f_i + f_{i+1}^p) \quad (15)$$

RESULTS AND DISCUSSION

The mathematical modeling of tumor growth and therapy helps us analyze the complex interactions between cancer cells, chemotherapy and immune cells with the objective of developing more efficient therapeutic modalities. In this study, we developed a system of ODEs to study the interactions between tumor cells and immune cells as well as chemotherapy. The system of ODEs was solved using three different methodologies, namely, the Runge-Kutta (RK) method, which was assumed to yield accurate values and accordingly was used as a reference, the Explicit Euler method, and Heun’s method. The results obtained using Euler’s explicit and Heun’s methods were then compared to the results obtained from the RK, and the percentage error for each was computed (the MATLAB code used to conduct the numerical analysis is given by Fig. 1). The estimated values of parameters used in the calculation are presented in Table I (as reported in the literature). Other initial conditions used were:

- The effect of immunotherapy through TIL drug intervention V_L is equal to 1×10^6 , and chemotherapy drug V_M is equal to 1.
- The level of chemotherapy drug kill terms (K) depends on how much cell division and growth are disrupted. If $K = 0$, the drug term will cancel out. For computational purposes, the drug kill term for the chemotherapeutic drug, dendritic cells, NK cells, and CD8+ T cells, respectively,

were set to $K_T = 9 \times 10^{-2}$, $K_D = 6 \times 10^{-2}$, $K_N = 6 \times 10^{-2}$, and $K_L = 6 \times 10^{-2}$.

- Time discretization Δt will be set to 0.5263 (days) for the proper visualization of changes in tumor cells, with a $T_{\text{max}} = 10$ days.

The percentage error to compare both the Explicit Euler method ($\%E_1$) and Heun’s method with the RK method ($\%E_2$) was calculated using the following two equations:

$$\%E_1 = \left| \frac{T_1 - T_2}{T_1} \right| * 100 \quad (16)$$

$$\%E_2 = \left| \frac{T_1 - T_3}{T_1} \right| * 100 \quad (17)$$

where T_1, T_2, T_3 are the values for tumor cells when the system is solved via the RK, Explicit Euler, and Heun’s methods, respectively. Tables III and IV present the values of tumor cells (T) for the 4 cases investigated. The values in Table II, calculated using the RK method, are used as a reference to compare the results obtained from the Explicit Euler method (Table III) and Heun’s method (Table IV), where the percentage errors for each were additionally calculated.

Figure 2 shows the tumor growth over time when: (1) there is no drug, (2) immunotherapy was administered, (3) chemotherapy was administered, and (4) a combination of chemotherapy and immunotherapy was administered. From Figure 2, it can be seen that the growth of tumor cells decreased over time when the combinational therapy was used, indicating that this modality was the optimal cancer treatment. Figure 3 shows the percentage error when comparing Euler Explicit and Heun’s with the reference RK method. The Heun’s method has a second-order error

Table II. Results using Runge-Kutta method.

n	Δt	T (No drug)	T (Immunotherapy)	T (Chemotherapy)	T (Immunotherapy & Chemotherapy)
0	0	100	100	100	100
1	0.5263	124.6796	124.5076	123.3744	123.2046
2	1.0526	153.5408	152.6986	148.1197	147.3137
3	1.5789	186.8072	184.5169	174.2171	172.1153
4	2.1052	224.5982	219.7436	201.6078	197.358
5	2.6315	266.9075	257.9791	230.1745	222.7372
6	3.1578	313.5809	298.6397	259.7386	247.9006
7	3.6841	364.302	340.9627	290.0667	272.4628
8	4.2104	418.5833	384.0268	320.8812	296.0237
9	4.7367	475.7648	426.7837	351.8717	318.1891
10	5.263	535.0229	468.1015	382.7089	338.5885
11	5.7893	595.3871	506.8183	413.0554	356.8912
12	6.3156	655.7677	541.7979	442.5777	372.8185
13	6.8419	714.9898	571.9911	470.9558	386.1527
14	7.3682	771.8355	596.4882	497.8916	396.7419
15	7.8945	825.0895	614.569	523.1157	404.502
16	8.4208	873.5863	625.7366	546.3932	409.4145
17	8.9471	916.257	629.7406	567.5265	411.5225
18	9.4734	952.1707	626.5836	586.3581	410.9249
19	9.9997	980.5713	616.5119	602.7713	407.7679

Table III. Results using explicit Euler method.

n	Δt	T (No drug)	True value	Percentage error %	T (Immunotherapy)	True value	Percentage error %	T (Chemotherapy)	True value	Percentage error %	T (Immunotherapy & Chemotherapy)	True value	Percentage error %
0	0	100	100	0.0000	100	100	0.0000	100	100	0.0000	100	100	0.0000
1	0.5263	122.6842	124.6796	1.6004	122.6842	124.5076	1.4645	122.6842	123.3744	0.5594	122.6842	123.2046	0.4224
2	1.0526	148.9661	153.5408	2.9795	148.6262	152.6986	2.6670	146.588	148.1197	1.0341	146.2481	147.3137	0.7234
3	1.5789	179.0379	186.8072	4.1590	177.8104	184.5169	3.6346	171.6834	174.2171	1.4543	170.4847	172.1153	0.9474
4	2.1052	213.0136	224.5982	5.1579	210.091	219.7436	4.3927	197.9229	201.6078	1.8278	195.1643	197.358	1.1115
5	2.6315	250.9096	266.9075	5.9938	245.1758	257.9791	4.9629	225.2119	230.1745	2.1560	220.0125	222.7372	1.2233
6	3.1578	292.6281	313.5809	6.6818	282.6162	298.6397	5.3655	253.401	259.7386	2.4400	244.7076	247.9006	1.2880
7	3.6841	337.9417	364.302	7.2358	321.8051	340.9627	5.6187	282.2881	290.0667	2.6817	268.8899	272.4628	1.3113
8	4.2104	386.4835	418.5833	7.6687	361.9851	384.0268	5.7396	311.6265	320.8812	2.8842	292.1776	296.0237	1.2993
9	4.7367	437.7417	475.7648	7.9920	402.2672	426.7837	5.7445	341.1357	351.8717	3.0511	314.1848	318.1891	1.2585
10	5.263	491.0616	535.0229	8.2167	441.6604	468.1015	5.6486	370.512	382.7089	3.1870	334.5396	338.5885	1.1958
11	5.7893	545.6543	595.3871	8.3530	479.1106	506.8183	5.4670	399.4408	413.0554	3.2961	352.9011	356.8912	1.1180
12	6.3156	600.6132	655.7677	8.4107	513.5481	541.7979	5.2141	427.6068	442.5777	3.3827	368.9731	372.8185	1.0314
13	6.8419	654.9382	714.9898	8.3989	543.939	571.9911	4.9043	454.704	470.9558	3.4508	382.5147	386.1527	0.9421
14	7.3682	707.5666	771.8355	8.3268	569.3387	596.4882	4.5516	480.4442	497.8916	3.5043	393.3484	396.7419	0.8553
15	7.8945	757.4093	825.0895	8.2028	588.9423	614.569	4.1699	504.5644	523.1157	3.5463	401.3629	404.502	0.7760
16	8.4208	803.3903	873.5863	8.0354	602.1283	625.7366	3.7729	526.8321	546.3932	3.5800	406.5141	409.4145	0.7084
17	8.9471	844.4885	916.257	7.8328	608.4925	629.7406	3.3741	547.05	567.5265	3.6080	408.8227	411.5225	0.6561
18	9.4734	879.7777	952.1707	7.6029	607.8689	626.5836	2.9868	565.0583	586.3581	3.6326	408.3686	410.9249	0.6221
19	9.9997	908.4634	980.5713	7.3537	600.336	616.5119	2.6238	580.736	602.7713	3.6557	405.2844	407.7679	0.6090

Table IV. Results using Heun's method.

n	Δt	Tc (No drug)	True value	Percentage error %	Tc (Immunotherapy)	True value	Percentage error %	Tc (Chemotherapy)	True value	Percentage error %	Tc (Immunotherapy & Chemotherapy)	True value	Percentage error %
0	0	100.0000	100.0000	0	100.0000	100.0000	0	100.0000	100.0000	0	100.0000	100.0000	0
1	0.5263	124.4830	124.6796	0.1577	124.3131	124.5076	0.1562	123.2940	123.3744	0.0652	123.1241	123.2046	0.0653
2	1.0526	153.0927	153.5408	0.2918	152.2639	152.6986	0.2847	147.9460	148.1197	0.1173	147.1451	147.3137	0.1144
3	1.5789	186.0496	186.8072	0.4056	183.7992	184.5169	0.3890	173.9359	174.2171	0.1614	171.8510	172.1153	0.1536
4	2.1052	223.4729	224.5982	0.5010	218.7042	219.7436	0.4730	201.2067	201.6078	0.1990	196.9926	197.3580	0.1851
5	2.6315	265.3574	266.9075	0.5808	256.5867	257.9791	0.5397	229.6436	230.1745	0.2307	222.2686	222.7372	0.2104
6	3.1578	311.5529	313.5809	0.6467	296.8716	298.6397	0.5921	259.0708	259.7386	0.2571	247.3297	247.9006	0.2303
7	3.6841	361.7490	364.3020	0.7008	338.8063	340.9627	0.6324	289.2580	290.0667	0.2788	271.7931	272.4628	0.2458
8	4.2104	415.4661	418.5833	0.7447	381.4802	384.0268	0.6631	319.9300	320.8812	0.2964	295.2612	296.0237	0.2576
9	4.7367	472.0545	475.7648	0.7799	423.8555	426.7837	0.6861	350.7795	351.8717	0.3104	317.3415	318.1891	0.2664
10	5.263	530.7018	535.0229	0.8076	464.8108	468.1015	0.7030	381.4789	382.7089	0.3214	337.6647	338.5885	0.2728
11	5.7893	590.4500	595.3871	0.8292	503.1930	506.8183	0.7153	411.6930	413.0554	0.3298	355.9009	356.8912	0.2775
12	6.3156	650.2221	655.7677	0.8457	537.8744	541.7979	0.7242	441.0900	442.5777	0.3361	371.7719	372.8185	0.2807
13	6.8419	708.8563	714.9898	0.8578	567.8118	571.9911	0.7307	469.3511	470.9558	0.3407	385.0601	386.1527	0.2829
14	7.3682	765.1469	771.8355	0.8666	592.1011	596.4882	0.7355	496.1794	497.8916	0.3439	395.6139	396.7419	0.2843
15	7.8945	817.8901	825.0895	0.8726	610.0254	614.5690	0.7393	521.3065	523.1157	0.3459	403.3487	404.5020	0.2851
16	8.4208	865.9305	873.5863	0.8764	621.0904	625.7366	0.7425	544.4978	546.3932	0.3469	408.2459	409.4145	0.2854
17	8.9471	908.2080	916.2570	0.8785	625.0470	629.7406	0.7453	565.5564	567.5265	0.3471	410.3482	411.5225	0.2854
18	9.4734	943.7987	952.1707	0.8793	621.8976	626.5836	0.7479	584.3248	586.3581	0.3468	409.7539	410.9249	0.2850
19	9.9997	971.9514	980.5713	0.8791	611.8882	616.5119	0.7500	600.6863	602.7713	0.3459	406.6089	407.7679	0.2842

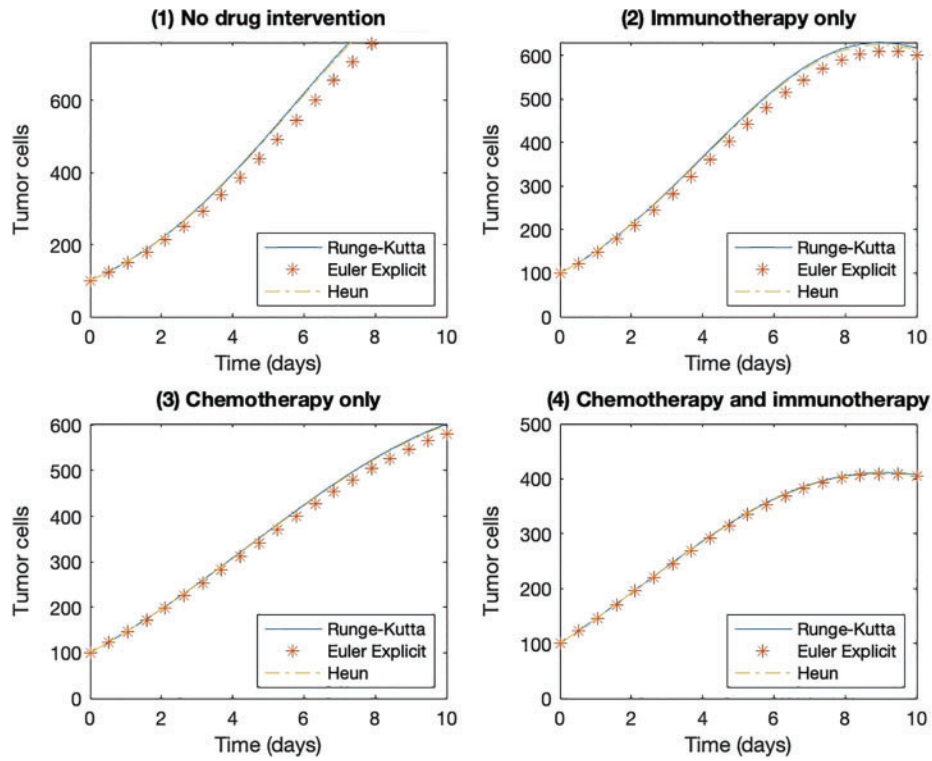


Figure 2. Modeling tumor dynamics using RK, Euler Explicit, and Heun's methods.

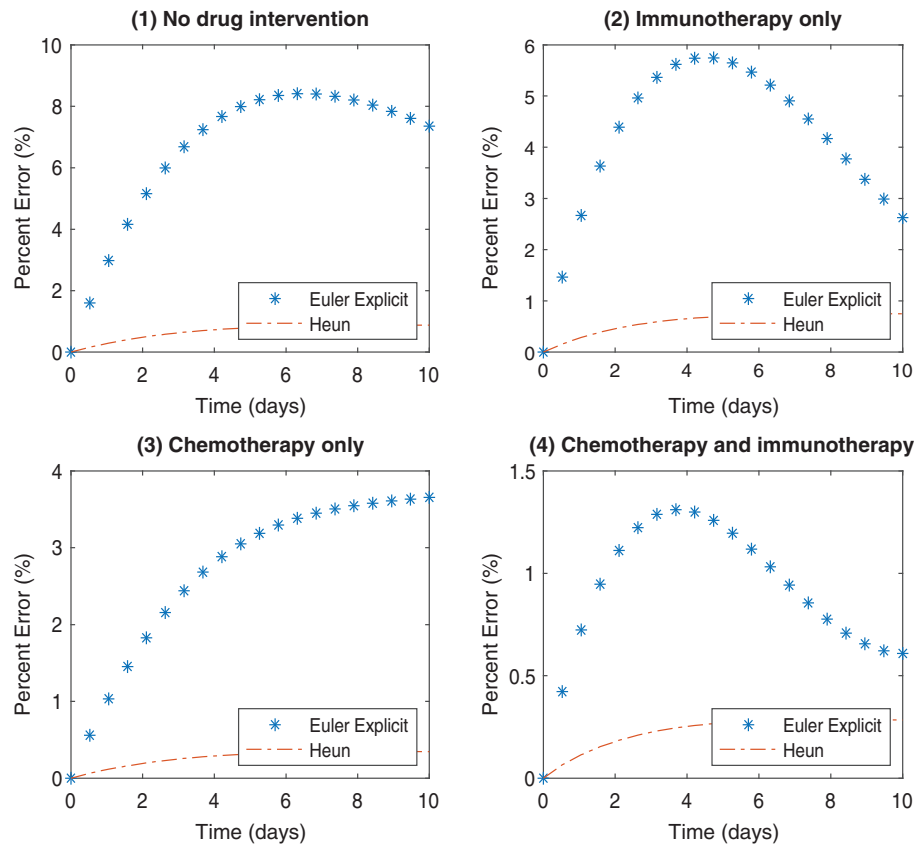


Figure 3. Percentage error of comparing Euler explicit and Heun's methods with the RK method.

Table V. Percentage error of explicit Euler using half the step size δt .

Percentage error with $\Delta t = 0.5263$	Percentage error with $\Delta t = 0.2632$
0	0
0.4224	0.2212
0.7234	0.3806
0.9474	0.5001
1.1115	0.5879
1.2233	0.6478
1.2880	0.6828
1.3113	0.6960
1.2993	0.6907
1.2585	0.6704
1.1958	0.6389
1.1180	0.5997
1.0314	0.5560
0.9421	0.5110
0.8553	0.4672
0.7760	0.4273
0.7084	0.3932
0.6561	0.3667
0.6221	0.3494
0.6090	0.3424

$O(h^2)$, whereas the Euler Explicit method has a first-order error $O(h)$. Accordingly, Heun’s method yielded lower percentage errors, meaning that the results were more accurate (closer to the true values obtained using the RK method). In order for Euler’s method to yield a similar accuracy to the RK method, smaller step sizes are required. For instance, if Euler’s accuracy must be improved a hundred-fold, it will need a hundred times as many steps, whereas Heun’s method would need only ten times as many steps to achieve a similar result. As seen in Table V above,

when the step size decreased from $\Delta t 0.5263 \rightarrow 0.2632$ the percentage error decreased as well. However, this may not always be the case, if too many small step sizes are used, errors might start to accumulate, and the estimated result may begin to diverge from the actual value. In addition, the conditioned stability when using Euler’s method (Table VI) must be taken into account. The percentage error for the explicit Euler method, at first, increased from counter $n = 0$ up to $n = 7$, then continued decreasing until the T_{max} was reached. These fluctuations show stability problems. Unlike Heun’s method which is unconditionally stable.

While mathematical models like the one we have developed and analyzed in this study have provided useful insights on the effectiveness of chemotherapy and immune therapy in treating cancer, there is still a great deal of research needed to enhance existing models and get them to a stage/phase where they can be incorporated into clinical work. For instance, there is still much that is not understood about tumor biology; in addition, cancer cells display a lot of phenotypic and genotypic variation, which introduces further complexity to any developed model [27]. With regard to immune cell components and their interactions with cancer cells, modeling using only one immune cell type yields models of limited utility and biological relevance, some models, similar to the one developed in this paper, incorporate several immune cell types to produce more realistic models. However, the more components introduced, the more complex it becomes, rendering it more computationally challenging and costly. The advent of omic data and machine learning has promise in addressing this issue. Moreover, further research is needed to understand the interactions between treatment modalities,

Table VI. Comparing tumor cells values (Immunotherapy & Chemotherapy intervention).

n	T (RK) true value	T (explicit Euler)	% Error (explicit Euler)	T_c (Heun’s method)	% Error (Heun’s method)
0	100	100	0	100	0
1	123.2046	122.6842	0.4224	123.1241	0.0653
2	147.3137	146.2481	0.7234	147.1451	0.1144
3	172.1153	170.4847	0.9474	171.851	0.1536
4	197.358	195.1643	1.1115	196.9926	0.1851
5	222.7372	220.0125	1.2233	222.2686	0.2104
6	247.9006	244.7076	1.2880	247.3297	0.2303
7	272.4628	268.8899	1.3113	271.7931	0.2458
8	296.0237	292.1776	1.2993	295.2612	0.2576
9	318.1891	314.1848	1.2585	317.3415	0.2664
10	338.5885	334.5396	1.1958	337.6647	0.2728
11	356.8912	352.9011	1.1180	355.9009	0.2775
12	372.8185	368.9731	1.0314	371.7719	0.2807
13	386.1527	382.5147	0.9421	385.0601	0.2829
14	396.7419	393.3484	0.8553	395.6139	0.2843
15	404.502	401.3629	0.7760	403.3487	0.2851
16	409.4145	406.5141	0.7084	408.2459	0.2854
17	411.5225	408.8227	0.6561	410.3482	0.2854
18	410.9249	408.3686	0.6221	409.7539	0.2850
19	407.7679	405.2844	0.6090	406.6089	0.2842

i.e., chemotherapy and immune therapy [27–29]. Another challenge for the practical application of these models is the collection of clinical data. Diagnostic data of cancer patients usually includes imaging and biopsy results; however, to assess the interactions and success of combination therapy (e.g., chemotherapy and immunotherapy), more complex information is needed. Even if such information were available, it would still be a challenge to incorporate into the models as meaningful parameters. Combinations of model systems would be one way to approach this issue, but that does not necessarily provide an ultimate solution [27, 28]. Expansion of the model to include additional patient tumor-specific information, such as genomic, transcriptomic and metabolomic data, might enhance system predictivity. In spite of these challenges, the ever-expanding biological knowledge of tumor-immune cell interactions coupled with the continuous advances in computational analysis paint a hopeful future for the practical application of relevant mathematical models with the ultimate goal of improving cancer therapies.

CONCLUSION

In this work, we developed a mathematical model to investigate the interactions between immune and tumor cells, study the effect of different treatments on tumor growth, as well as compare different mathematical approaches commonly used in modeling tumor growth, namely the Runge-Kutta method, the explicit Euler's method and Heun's method. Moreover, a stability analysis of the developed ODEs is provided to ensure the results are meaningful near the equilibrium point. Our results showed that the combination of immunotherapy and chemotherapy decreased tumor growth, and that the Heun's method provided the closest accuracy to the true value given by the Runge-Kutta output. Future work may include a system of partial differential equations that models the fluid transport in the tumor region and helps the drugs target the tumor cell, as well as a study of the interactions between the investigated cell populations, and how their interactions would affect the developed model.

Conflicts of Interest

There are no conflicts to declare.

Acknowledgments: The authors would like to acknowledge the American University of Sharjah Faculty Research Grants (FRG20-L-48, and eFRG18-BBRCEN-03), and Sheikh Hamdan Award for Medical Sciences (Grant number MRG-57-2019-2020).

REFERENCES

- American Cancer Society. Cancer Facts and Figures 2021. (<https://www.cancer.org/content/dam/cancer-org/research/cancer-facts-and-statistics/annual-cancer-facts-and-figures/2021/cancer-facts-and-figures-2021.pdf>).
- PLOS medicine editors. 2015. Bringing access to the full spectrum of cancer research: A call for papers. *PLoS Med*, 12(4), p.e1001817, DOI: 10.1371/journal.pmed.1001817.
- Wasteson, E., Brenne, E., Higginson, I.J., Hotopf, M., Lloyd-Williams, M., Kaasa, S., Loge, J.H., and European Palliative Care Research Collaborative (EPCRC), 2009. Depression assessment and classification in palliative cancer patients: A systematic literature review. *Palliative Medicine*, 23(8), pp.739–753.
- Konfortion, J., Jack, R.H. and Davies, E.A., 2014. Coverage of common cancer types in UK national newspapers: A content analysis. *BMJ Open*, 4(7), p.e004677.
- Blackadar, C.B., 2016. Historical review of the causes of cancer. *World Journal of Clinical Oncology*, 7(1), p.54.
- Boujelbene, N., Cosinschi, A., Boujelbene, N., Khanfir, K., Bhagwati, S., Herrmann, E., Mirimanoff, R.O., Ozsahin, M. and Zouhair, A., 2011. Pure seminoma: A review and update. *Radiation Oncology*, 6(1), pp.1–12.
- Yin, A., Moes, D.J.A., van Hasselt, J.G., Swen, J.J. and Guchelaar, H.J., 2019. A review of mathematical models for tumor dynamics and treatment resistance evolution of solid tumors. *CPT: Pharmacometrics & Systems Pharmacology*, 8(10), pp.720–737.
- Valentim Jr., C.A., Oliveira, N.A., Rabi, J.A. and David, S.A., 2020. Can fractional calculus help improve tumor growth models? *Journal of Computational and Applied Mathematics*, 379, p.112964.
- Ucar, E., Özdemir, N. and Altun, E., 2019. Fractional order model of immune cells influenced by cancer cells. *Mathematical Modelling of Natural Phenomena*, 14(3), p.308.
- Khajanchi, S. and Nieto, J.J., 2019. Mathematical modeling of tumor-immune competitive system, considering the role of time delay. *Applied Mathematics and Computation*, 340, pp.180–205.
- Peng, C., Liu, L.Z., Zheng, W., Xie, Y.J., Xiong, Y.H., Li, A.H. and Pei, X.Q., 2016. Can quantitative contrast-enhanced ultrasonography predict cervical tumor response to neoadjuvant chemotherapy? *European Journal of Radiology*, 85(11), pp.2111–2118.
- Patwardhan, G., Gupta, V., Huang, J., Gu, X. and Liu, Y.Y., 2010. Direct assessment of P-glycoprotein efflux to determine tumor response to chemotherapy. *Biochemical Pharmacology*, 80(1), pp.72–79.
- Zhao, J., Krishnamurti, U., Zhang, C., Meisel, J., Wei, Z., Suo, A., Aneja, R., Li, Z. and Li, X., 2020. HER2 immunohistochemistry staining positivity is strongly predictive of tumor response to neoadjuvant chemotherapy in HER2 positive breast cancer. *Pathology-Research and Practice*, 216(11), p.153155.
- Anaya, D.A., Dogra, P., Wang, Z., Haider, M., Ehab, J., Jeong, D.K., Ghayouri, M., Lauwers, G.Y., Thomas, K., Kim, R. and Butner, J.D., 2021. A mathematical model to estimate chemotherapy concentration at the tumor-site and predict therapy response in colorectal cancer patients with liver metastases. *Cancers*, 13(3), p.444.
- Koziol, J.A., Falls, T.J. and Schnitzer, J.E., 2020. Different ODE models of tumor growth can deliver similar results. *BMC Cancer*, 20(1), pp.1–10.
- Aghaei, F., Tan, M., Hollingsworth, A.B. and Zheng, B., 2016. Applying a new quantitative global breast MRI feature analysis scheme to assess tumor response to chemotherapy. *Journal of Magnetic Resonance Imaging*, 44(5), pp.1099–1106.
- Ledzewicz, U., Naghnaean, M. and Schättler, H., 2012. Optimal response to chemotherapy for a mathematical model of tumor-immune dynamics. *Journal of Mathematical Biology*, 64(3), pp.557–577.
- Alvarez, R.F., Barbuto, J.A. and Venegeroles, R., 2019. A nonlinear mathematical model of cell-mediated immune response for tumor phenotypic heterogeneity. *Journal of Theoretical Biology*, 471, pp.42–50.
- Admon, M.R. and Maan, N., 2017. Modelling tumor growth with immune response and drug using ordinary differential equations. *Jurnal Teknologi*, 79(5).

20. Pinho, S.T.R.D., Bacelar, F.S., Andrade, R.F.S. and Freedman, H.I., **2013**. A mathematical model for the effect of anti-angiogenic therapy in the treatment of cancer tumours by chemotherapy. *Nonlinear Analysis: Real World Applications*, *14*(1), pp.815–828.
21. Unni, P. and Seshaiyer, P., **2019**. Mathematical modeling, analysis, and simulation of tumor dynamics with drug interventions. *Computational and Mathematical Methods in Medicine*.
22. Robertson-Tessi, M., El-Kareh, A. and Goriely, A., **2015**. A model for effects of adaptive immunity on tumor response to chemotherapy and chemoimmunotherapy. *Journal of Theoretical Biology*, *380*, pp.569–584.
23. Curtis, L.T. and Frieboes, H.B., **2019**. Modeling of Combination Chemotherapy and Immunotherapy for Lung Cancer. *2019 41st Annual International Conference of the IEEE Engineering in Medicine and Biology Society (EMBC)*, IEEE, pp.273–276.
24. Gun, S.Y., Lee, S.W.L., Sieow, J.L. and Wong, S.C., **2019**. Targeting immune cells for cancer therapy. *Redox. Biol.*, *25*, p.101174.
25. Mahlbacher, G.E., Reihmer, K.C. and Frieboes, H.B., **2019**. Mathematical modeling of tumor-immune cell interactions. *Journal of Theoretical Biology*, *469*, pp.47–60.
26. Workie, A.H., **2020**. New modification on heun's method based on contraharmonic mean for solving initial value problems with high efficiency. *Journal of Mathematics*, *2020*.
27. Bruno, R., Bottino, D., De Alwis, D.P., Fojo, A.T., Guedj, J., Liu, C., Swanson, K.R., Zheng, J., Zheng, Y. and Jin, J.Y., **2020**. Progress and opportunities to advance clinical cancer therapeutics using tumor dynamic models. *Clinical Cancer Research*, *26*(8), pp.1787–1795.
28. Yousef, A., Bozkurt, F. and Abdeljawad, T., **2020**. Mathematical modeling of the immune-chemotherapeutic treatment of breast cancer under some control parameters. *Advances in Difference Equations*, *2020*(1), pp.1–25.
29. Aggarwal, B.B., Danda, D., Gupta, S. and Gehlot, P., **2009**. Models for prevention and treatment of cancer: Problems vs. promises. *Biochemical Pharmacology*, *78*(9), pp.1083–1094.